Bayero Journal of Physics and Mathematical Sciences / Vol. 16, No. 2 / Nov., 2025. ISSN: 1597 – 9342, Online ISSN: 2795 - 3866

BAJOPMAS JOURNAL 16(1): 80 – 92
Printed in Bayero University, Kano - Nigeria.

STRUCTURAL DEPTH INTERPRETATION FOR GOLD EXPLORATION USING AEROMAGNETIC DATA IN WESTERN PARTS OF ZAMFARA, NORTHWESTERN NIGERIA.

[1,2*]Sani, A. A.; [2]Aku, M. O.; [2]Saleh, M. and [3]Bagare, A. A.
[1]Federal University Birnin Kebbi
[2]Bayero University Kano
[3]Yobe State University
[*]Corresponding author: Aminu Abubakar Sani[1], aa.sani@fubk.edu.ng

ABSTRACT
The structural depth interpretation of magnetic sources associate with gold and its proxy minerals was carry out in the western parts of Zamfara, Nigeria, using aeromagnetic data. The research area has been formerly explored for solid minerals using assortments of anaylsis, however there was no focus on the influence of enhancement filters such as the CET Porphyry on the depth and structures (Euler 3D) that houses gold and its proxy. This research subject the total magnetic intensity grid to produce Reduce to equator, residual grid, Tilt derivative, Lineament, Porphyry CET, Euler deconvolution and Source Parameter imaging. The Tilt derivative Map revealed the linear features (faults, fractures and shear zones) trending NS, NE and WE of the study area. The geological features that supports the existence of gold and associate minerals has been outlined clearly in all the maps. There are good similarities in term of geology, lineament and porphyry deposit maps of gold mines site and gold prospect zones. The result revealed six (6) prospect zones which are *sunke of Anka area, Surimi of Bukkuyum, Mai iwa of Dangulbi, Birnin Magaji, Leshi and Gayawa of Gummi area.* The Euler depth solution for contact/step models (Structural Index = 0) show the contact zone around Northern parts of *Gummi, Anka and western part of Talata Mafara* area between basement complex and sedimentary basin with an average depth estimated from 100m -700m. For the dyke and sill model of structural index 1, for Pipe and cylinder model of structural index 2 and sphere model of structural index 3 has shown a positive correlation with geology, lineament and porphyry maps of the study area. The solutions have clustered at places with major faults and fractures with an estimated average depth 100m – 700m that coincide with gold and associate minerals deposits.

Keywords: Aeromagnetic data, Euler, Gold, Lineaments, Nigeria, Northwestern, Porphyry CET, Tilt derivatives, Western part, Zamfara.

1.0 INTRODUCTION
Aeromagnetic survey is the common type of geophysical survey and has been recognized as a major tool for mapping materials that are strongly magnetized [1]. Magnetic method seeks to study the geology of the particular area due to the differences in the earth magnetic field. These differences are as a result of the magnetic features of subsurface rocks [2]. The most vital magnetic minerals in soils are the iron oxides, such as magnetite. In mineral exploration, the magnetic data can be used to solve different problems in many ways depending on the geologic setting and rock constraints [3]. Moreover, magnetic data can be processes and analyzed to provide an insight to the element of mineral exploration [4]. The magnetic enhancement filters has a curiosity that it is a fast and adequate technique for investigating the subsurface geological structures (faults, folds, fractures and shear zone), geothermal potentials and delineating the basement structures [5,6,7,8,9]. The method also

provides an insight into mapping basement surfaces and delineating the subsurface structures that coincide with gold and associate minerals.

Gold is a precious metal of high commercial value and great economic importance [10]. Gold is generally found in Nigeria as alluvial and eluvial placers and primary veins from several parts of supracrustal (schist) belts, in the northwest and southwest of the country [11]. The gold mineralization is associated with veins, stringers, lenses, reefs and similar bodies of quartz, quartz-feldspar and quartz-tourmaline rocks in both the supracrustal rocks and basement [12]. The quartz veins containing gold occur in association with metamorphosed rocks ranging in composition from semi pelitic to pelitic and mafic [13]. Primary gold mineralization produced chemical signature in the overburden and surrounding soil probably through weathering processes [14].

Numerous researchers have investigated in Zamfara concerning its gold mineralisation, including [10] and [15]. [10] Used first vertical and second vertical derivatives on aeromagnetic data to analyze gold prospects in Anka schist belt. While [15] used geochemical analysis to interpreted trace elements to characterize some of the features that are diagnostic of the origin of gold deposits. Although the research by [10] reveal some structural trends, significant improvements could be made by applying more advance and automated techniques such as the CET. Furthermore his method fail to address the depth and structure of the interpreted features which could be clearly identified via the Euler technique. Moreover, the research by [15] identify some traces of gold minerals, his techniques involves sampling of few rocks which is not feasible to cover a very large area such as our study area. Therefore, this study is aimed to delineating gold and associated minerals prospect in the western part of the zamfara state, north western Nigeria using aeromagnetic data. This research seeks to review the geology and to aid the delineation of regional and local geological structures (shear zones and faults) and the depth of anomalous body that may hosts gold and associate minerals within the study area. The techniques was applied are reduce to magnetic equator, residual map, tilt derivative map, lineament, CET porphyry, euler deconvolution and sources parameter imaging respectively. The effort allows the estimate of target areas for detailed exploration.

2.0 Location and Geology of the Study Area

The study area is bounded by the longitudes $5^{o}00^{'}E$ to $6^{o}30^{'}E$ and latitudes $11^{o}30^{'}N$ to $13^{o}00^{'}N$ and it occupies an area of 165 km by 165 km ($27{,}223km^{2}$) located in western part of Zamfara state established with sedimentary basin and basement complex regions. The part of the study area is the basement complex which was affected by the Pan-African orogeny. The Basement Complex of Nigeria consists of migmatites and migmatitic gneisses, slightly migmatized to unmigmatized paraschists with interbeds of meta and non-meta-igneous rocks, also referred to as the younger metasediments or the Schist belts and the older Granite suite comprising mainly different varieties of granitic rocks/granitoids [16]. The rocks contrast within include metaconglomerates, sandstones, slates, phyllites and acid volcanic rocks [17,18]. The major rocks occurred dominated area are granite gneiss, medium to coarse grained biotite granite, carbonaceous and undifferentiated schist including phyllite and minor rocks are metaconglomerate, migmatite, Alluvium, pegmatite and rhyolite all in Danko, bukkuyum, Dangulbi, Anka, Maru and some part of Gummi, Talata mafara of Anka and Maru Schist belts. The sandstone, siltstone, shale, gravel, sand, clay grit and pebbles rocks are all in Dange, Gandi and some parts of the Gummi and Talata mafara of sedimentary terrain (Fig. 1).

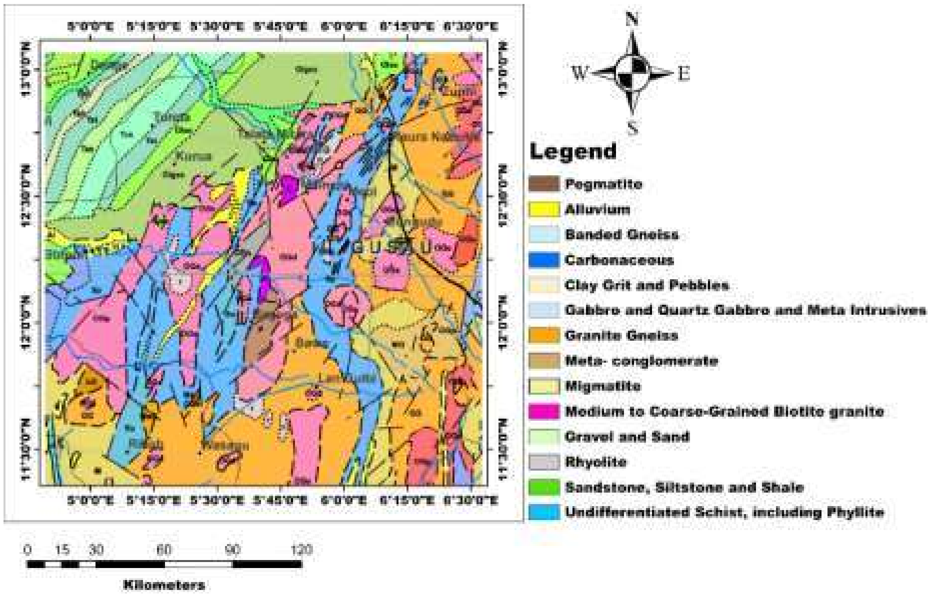

Figure 1 Geology map of the study Area

3.0 MATERIALS AND METHOD

The materials and method used in this research are described below.

3.1 Data Acquisition

A high resolution aeromagnetic datasets of sheets number 29, 30, 31, 51, 52, 53, 74, 75 and 76 covered Dange, Gandi, Talata Mafara, Gummi, Anka, Maru, Danko, Bukkuyum and Dan Gulbi sheets were used in this study. The data was acquired from the Nigerian Geological Survey Agency. Data acquisitions were carried out with fixed wing Cessna aircrafts, with mean terrain clearance of 80m, measurements were recorded at an interval of 0.1 seconds or less. Flight lines spacing is 500 m with a trend of 135° (NW-SE), while tie lines spacing is 5km, with a trend of 45°. The pre-processed data was provided by the NGSA as a 2D grid of total magnetic intensity (TMI), with constant cell spacing of 100 m. The IGRF 2005 model was used in calculation of declination and inclination, since the data was collected from 2005 and 2009. The geographic coordinate system and WGS 84 reference datum were used during data acquisition and pre-processing. The coordinate system was however transformed to the UTM Zone 32N Cartesian coordinate system prior to processing. A value of 33,000 nT was added to the TMI data as this was removed initially from the field data during pre-processing.

3.2. Data Processing

The aeromagnetic data was further processed, enhanced and analyzed with Geosoft (Oasis Montaj), ArcGIS and Surfer software. The two-dimensional Fast Fourier Transform (2D-FFT) in MAGMAP is particularly useful in the transformation from the frequency domain to the wave number domain and also for the calculation of derivatives [19]. In this research, filters that were used of enhanced the magnetic data included reduction to magnetic equator, residual map , tilt derivative, center for exploration target (CET), porphyry (CET), sources parameter imaging and euler deconvolution.

3.2.1 Reduction to Equator (RTE)

This operation transforms the observed total magnetic intensity (TMI) into anomaly that would have been measured if the magnetization and ambient field were both horizontal. It is therefore possible to have magnetic anomalies over their causative source to facilitating the interpretation of geological features [20].

3.2.2 The Regional – Residual Separation

Aeromagnetic data observed in geophysical surveys are the sum of magnetic fields produced by all subsurface sources. The targets for specific surveys are often small-scale structures buried at shallow depths, and the magnetic responses of these targets are embedded in a regional field that arises from magnetic sources that are usually larger or deeper than the targets. Correct estimation and removal of the regional field from the initial field observations yields the residual field produced by the target sources. Analysis and numerical modeling are carried out on the residual field data, and the reliability of the interpretation depends to a great extent upon the success of the regional-residual separation [21]. Polynomial fitting was applying to total magnetic intensity map for regional and residual separation.

3.2.3 The Tilt Derivative Technique

The tilt derivative is a geometrical function of the vertical and horizontal derivatives of the field. It is also useful for mapping shallow basement structures and mineral exploration targets [22].
The tilt derivative is defined as:

$$\text{TDR} = \tan^{-1}\left(\frac{VDR}{THDR}\right) \qquad (1)$$

3.2.4 The Centre for Exploration Target (CET)

The CET Analysis contained tools for texture analysis, lineation detection, lineation vectorization and structural complexity. These are versatile algorithms useful for grid texture analysis, lineament detection, edge detection, thresholding, and identifying areas of structural complexity. Standard deviation provides an estimate of the local variation in the data. At each location in the grid, it calculates the standard deviation of the data values within the local neighbourhood. Features of significance often exhibit high variability with respect to the background signal [23]

$$\sigma = \sqrt{\frac{1}{N}\sum_{i=1}^{N}(x_i - \mu)^2} \qquad (2)$$

where σ is a standard deviation, N is cell, μ is a mean value and x_i is the cell values of the standard deviation.

3.2.5 Porphyry (CFT)

The CFT Porphyry Analysis Extension includes: the circular feature transform plugin, the central peak detection plugin, the Amplitude contrast transform plugin and the Boundary tracing plugin. This detection techniques locates and outlines circular zonation shapes in the magnetic data that associated with the central intrusion and inner alteration zone of the porphyry system. It is useful for detecting anomalies that coincide gold and copper porphyry especially in basement complex terrain

3.2.6 Euler Depth Determination Techniques

The determination of the depth to the major structures outlined prompt for the use of Euler's deconvolution algorithm. The acquaintance of these depths will aid in the ease of exploration of available minerals. Euler's depth has a special advantage over other depth estimation method; it targets the centre to the anomaly of interest rather than depth of overburden of the field and it employs the structural index for each of the anomaly targeted, equally its degree of accuracy can be improved by filtering its results. A formulation of Euler's homogeneity relationship given by (eq. 3) [24].

$$(x - x_0)\frac{\delta T}{\delta x} + (y - y_0)\frac{\delta T}{\delta y} + (z - z_0)\frac{\delta T}{\delta z} = N(B - T) \quad (3)$$

where *(x_0, y_0 and z_0)* are the magnetic source positions whose entire magnetic intensity field T is ascertained at *(x, y, z).* The total field with a regional value of B. N represents a structural index.

The structural index values and geometry are contact/step with SI = 0, sill/dyke with SI = 1, cylinder/pipe with SI = 2 and sphere/barrel with SI = 3 [24].

3.2.7 Source Parameter Imaging

The Source Parameter Imaging (SPI) technique is a procedure for automatic calculation of source depths from gridded magnetic data. These depth results are independent of the magnetic inclination and declination [25]. SPI assumes a step-type source model. For a step, the following formula holds:

$$\text{Depth} = \frac{1}{Kmax} \quad (4)$$

where Kmax is the peak value of the local wavenumber K over the step source.

4.0 RESULTS AND DISCUSSION

The results of the structural depth interpretation of magnetic sources associate with gold and its proxy minerals using aeromagnetic data is presented below.

4.1.1 Total Magnetic Intensity Map

The total magnetic intensity map of western part of Zamfara state, Nigeria after the add 33,000 nT which was initial removed by International Geomagnetic Reference Field (IGRF) is displayed (Fig. 2.) The map is grouped into colour aggregate, with blue to cyan depicting low magnetic anomalies while green to red depicts intermediate magnetic anomalies whereas pink colour depicts high magnetic anomalies. The Total Magnetic Intensity map of the study area in figure 2 displays both considerable low, intermediate and high anomalies ranging from 32905 nT to 33119 nT.

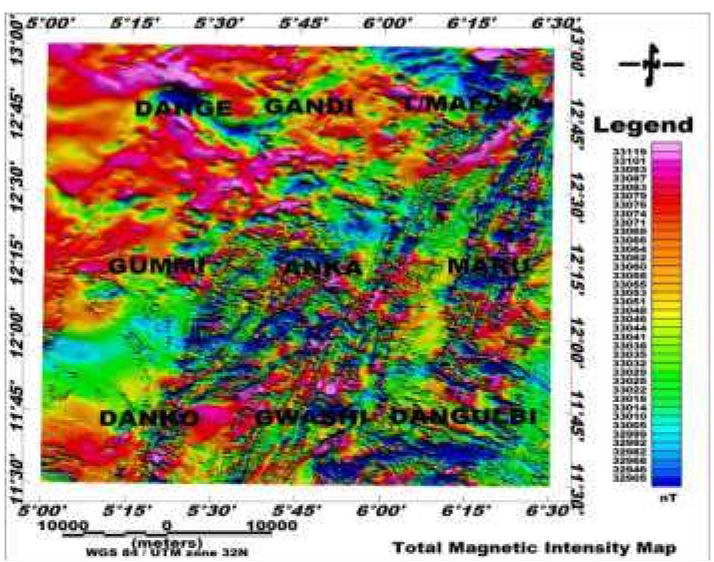

Figure 2: Total Magnetic Intensity Map

4.1.2 Reduced to Equator (RTE) and Residual Anomaly Map

The study area is in low magnetic latitude, to identify the observed magnetic anomalies directly over the magnetic source bodies, then total magnetic intensity (TMI) grid was transformed into reduction to the magnetic equator (RTE) grid using the 2D-FFT filter. The magnetic inclination (− 1.36) and declination (− 2.83) were obtained based on the International Geomagnetic Reference Field (IGRF) 2006 on the magnetic calculator to produce the reduction to the magnetic equator (RTE) map. This map of RTE (Fig. 3) sharpens the contacts between the magnetic high and low patterns as well as anomalously high magnetic zones. Moreover, the regional-residual separation was performed an obtained the residual map using the least squares polynomial fitting technique for the further analysis (Fig. 4).

4.1.3 Tilt Derivative and Lineament (CET) Map

The residual anomaly map was analysed to tilt derivative map (Fig. 5). The observed anomalies on the Tilt derivative Map (Fig. 5) are clearly different to that observed from (Fig. 2, 3 and 4). The linear features are clearly revealed compared to (Fig. 2, 3 and 4) the faults, fractures and shear zones trend NS NE and WE of the study area. The Tilt derivative values ranges from -1.330 to 1.384 rad/m and shows a large contrast in magnetic susceptibility along geologic contacts. Furthermore, the Centre for Exploration Targeting (CET) has advantages over derivative filters because CET being an automatic method even small lineament in a large area that may escape visual observation was observed. There are good correlation between CET lineaments map (Fig. 6) and tilt derivative map (Fig. 5). The result (Fig. 6) shows the occurrence of several lineaments predominantly trending in the NS- NE and WE directions. This gives further evidence of the extent of deformation that occurred within the study area.

4.1.4 Porphyry CET Map

The Porphyry CET revealed rocks that are porphyritic containing small and large crystals, a specific deposit containing widely disseminated metals, typically copper, gold and silver. This technique were applied to residual map (Fig. 4), at CET Porphyry Analysis algorithm that includes the circular feature transform plugin, the central peak detection plugin, the Amplitude contrast transform plugin and the Boundary tracing plugin. This detection techniques locates and outlines circular zonation shapes in the magnetic data that associated with the target of interest. The study area have abundant of porphyry deposits (Fig. 7). The correlation between published geology map and porphyry map of the study area, revealed predominately porphyry except around Dange, Gandi and some parts of the Talata mafara and Gummi. The major rocks occurred in porphyry dominated area are granite gneiss, medium to coarse grained biotite granite, carbonaceous and undifferentiated schist including phyllite and minor rocks are metaconglomerate, migmatite, Alluvium, pegmatite and rhyolite all in Danko, bukkuyum, Dangulbi, Anka, Maru and some part of Gummi, Talata mafara of Anka and Maru Schist belts. The sandstone, siltstone, shale, gravel, sand, clay grit and pebbles rocks are all in Dange, Gandi and some parts of the Gummi and Talata mafara of sedimentary terrain.

4.1.5 Euler Deconvolution and Sources Parameter Map

The depth to magnetic sources were estimated using euler deconvolution and source parameter imaging. The Standard Euler Deconvolution technique was implemented to the residual grid in order to obtain depth to magnetic sources. Four Structural Indices (SI) were adopted in this study; SI = 0 for contact model (Fig. 8), SI=1 for Dike and Sill models (Fig. 9), SI=2 for Pipe and horizontal/vertical cylinder models (Fig. 10) and SI = 3 for sphere and barrel models (Fig. 11). This was done in order to obtain well-informed depth information of magnetic materials within the study area. For all models, a window size of 20 and maximum depth tolerance of 5 % were assumed. From the four maps, the depths to magnetic source within the area are categorized in to five (5) sections red colour area less than 100m, blue colour 100m-300m , green colour 300m-500, yellow colour 500m-700m and pink colour greater than 700m respectively. There are positive correlation between obtained Euler depth and Source parameter imaging depth (Fig. 12), the depth obtained from SPI ranged from 80m – 742m which are similarly obtained from euler solution.

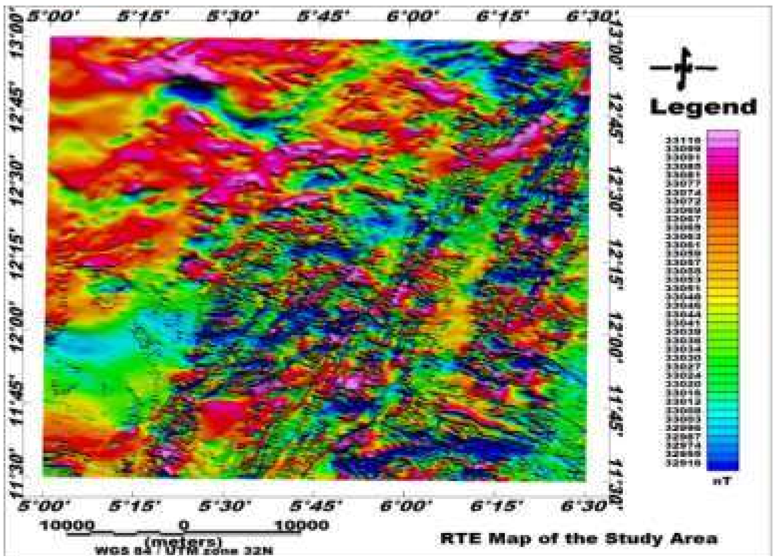

Figure 3 Reduction to the Magnetic Equator Map

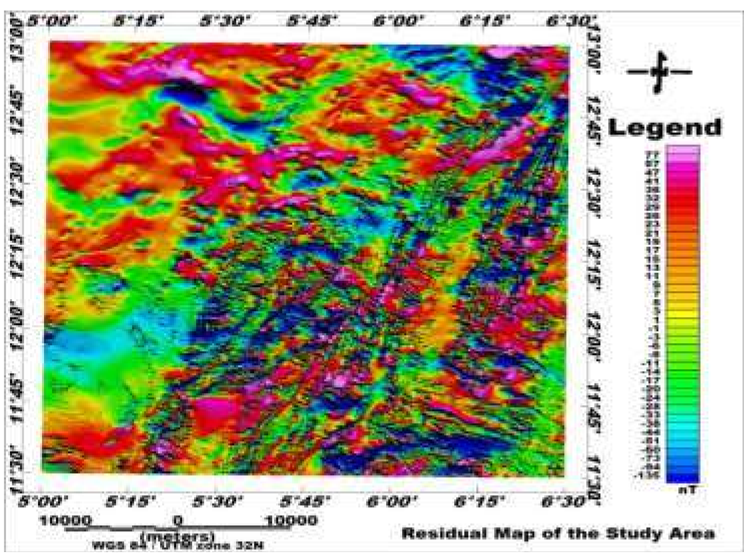

Figure 4 Residual Map of the Study Area

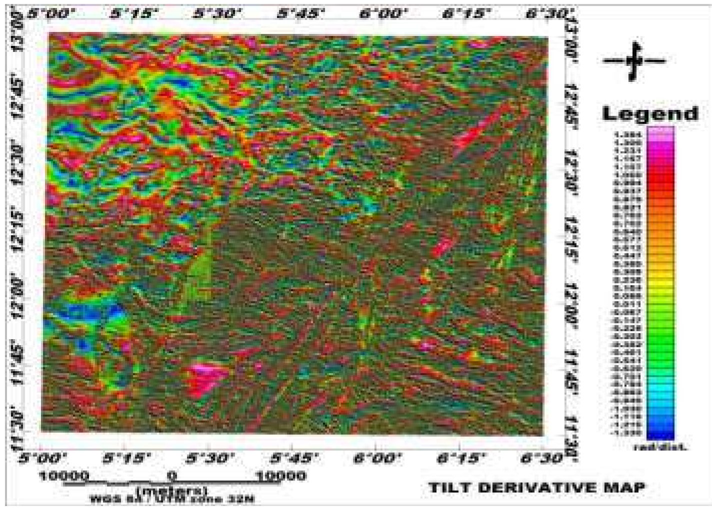

Figure 5 Tilt Derivative Map of the Study Area

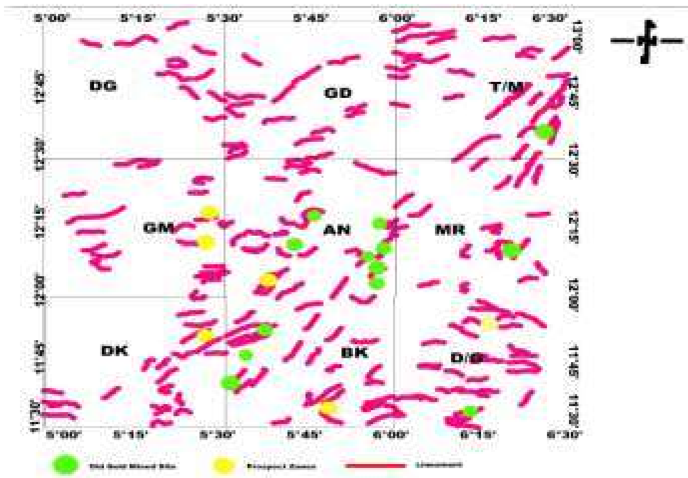

Figure 6 Lineament Map CET of the Study Area

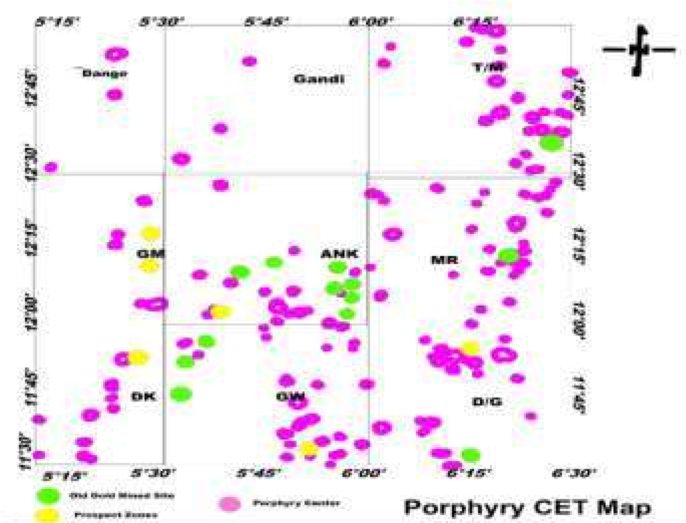

Figure 7 Porphyry CET Map of the Study Area

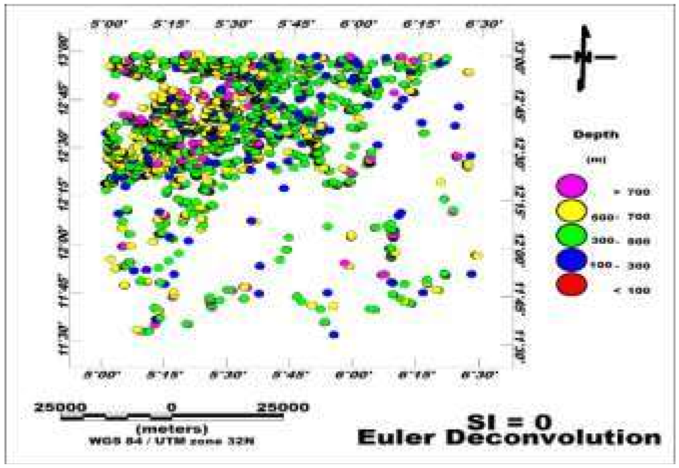

Figure 8 Euler Deconconvolution Map of the Study Area

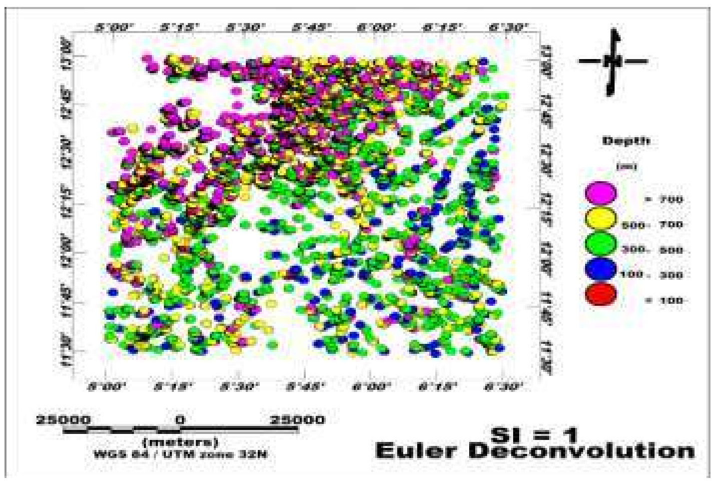

Figure 9 Euler Deconconvolution Map of the Study Area

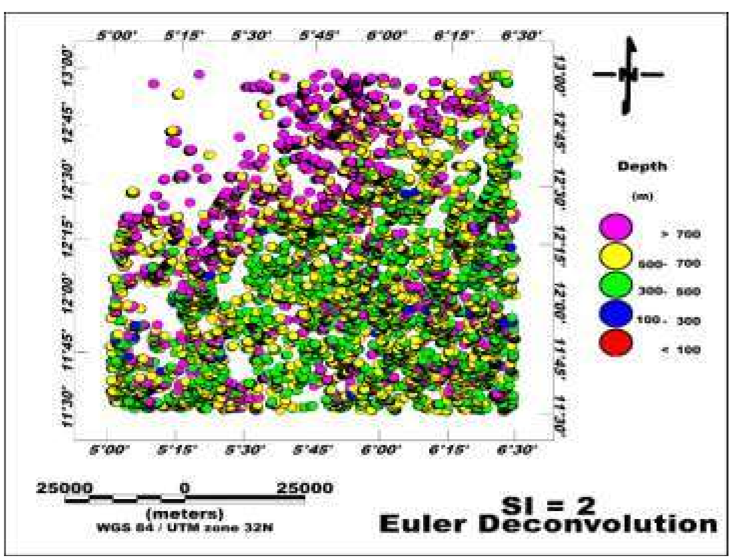

Figure 10 Euler Deconconvolution Map of the Study Area

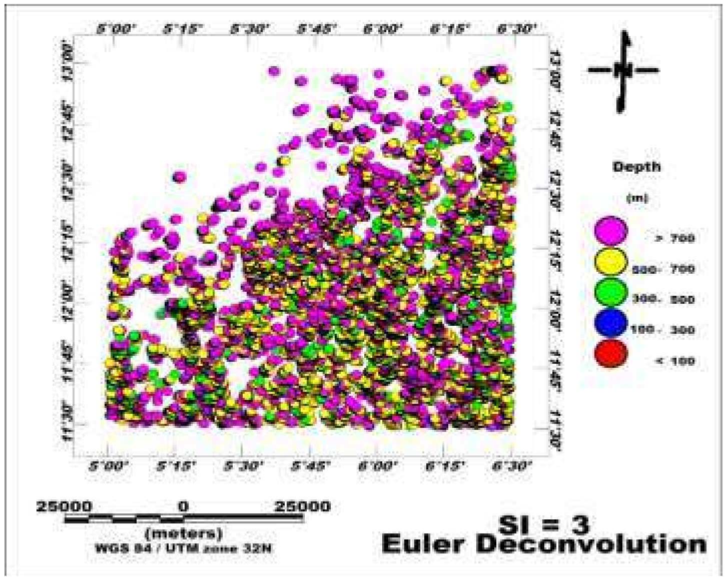

Figure 11 Euler Deconconvolution Map of the Study Area

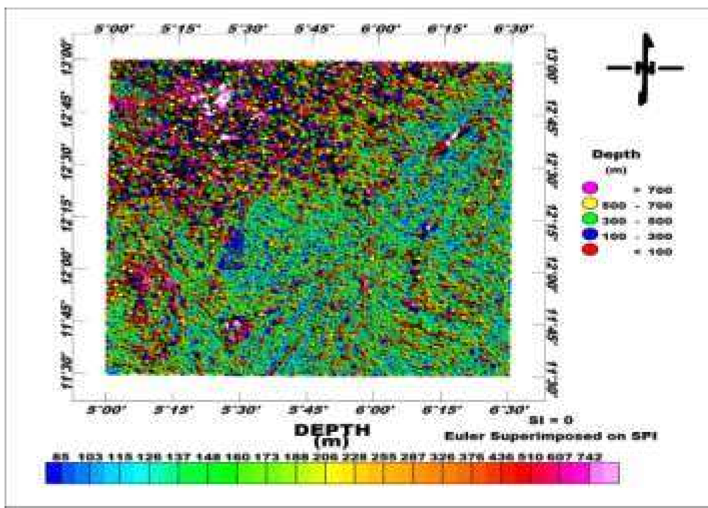

Figure 12 SPI map of the Study Area

4.2 Discussion

The results have all shown resemblances in the structures of the subsurface. The lineament map is very much in good correlation with the geological map and the porphyry map. The geological features that supports the existence of gold and associate minerals has been outlined clearly in all the maps, the existing gold mines site and prospects zones have similarities in lithology and geological structures. There are good agreement between gold mines site and processed maps (Fig. 1, 6 and 7) in which green colour represent gold mines site and yellow colour represent gold prospect zones. The previous study showed that gold mineralization occured at Kuba I, Kuba II, Doka, Dumi I, Dumi II, Zurzurfa I, Zurzurfa II, Jameson, Kwali and Kuba Mansur areas of the Anka schist belt [15]. Furthermore, another gold mines site during our field are the eastern part of Maru, Yargalma , Tudun guru and Gayawa in Bukkuyum area. Maga, Zugu in Danko area and Mairairai in Dangulbi area. There are good similarities in term of geology, lineament and porphyry deposit maps of gold mines site and gold prospect zones. The prospecting zones are sunke of Anka area, Surimi of Bukkuyum, Mai iwa of Dangulbi and Birnin Magaji, Leshi and Gayawa of Gummi area, these areas have structures (faults, fractures and shear zones) and depths of existing mine site.

The four Euler depth solution, the solution for contact/step models (Structural Index = 0) in Figure 8 show the contact zone around Northern parts of Gummi, Anka and western part of Talata Mafara area between basement complex and sedimentary basin with an average depth estimated from 100m -700m. For the dyke and sill model (figure 9) of structural index 1, for Pipe and cylinder model (figure 10) of structural index 2 and sphere model (figure 11) of structural index 3 has shown a positive correlation with (Fig. 1, 6 and 7) maps. The solutions have clustered at places with major faults and fractures with an estimated average depth 100m – 700m that coincide with gold and associate minerals deposits. The Pipe and cylinder model (figure 10) of structural index 2 is more favorable for gold deposits.

5.0 CONCLUSION

The aeromagnetic data have been processed and analyzed to understand geological structures and depth of magnetic sources that coincide of gold and associate minerals of western part of Zamfara North western Nigeria. A variety of enhancement techniques were applied to TMI grid. The total magnetic intensity (TMI) grid was transformed into reduction to the magnetic equator (RTE) grid. Moreover, the regional-residual separation was performed an obtained the residual map, the residual map was analysed to tilt derivative map. The Tilt derivative Map is revealed the linear features (faults, fractures and shear zones) trend NS NE and WE of the study area. The Tilt derivative values ranges from -1.330 to 1.384 rad/m and shows a large contrast in magnetic susceptibility along geologic contacts. The lineament was automatically extracted from residual grid. The map shows the occurrence of several magnetic deep sources crossing lineaments predominantly trending in the NS- NE and WE directions. This gives further evidence of the extent of deformation that occurred within the study area. Furthermore Porphyry CET was applied to residual grid where porphyry deposit are detected. The correlation between previous work and present work, gold mines site and prospect zone identified in different locations.

The depth to magnetic sources were estimated using euler deconvolution and source parameter imaging. Four Structural Indices (SI) were adopted in this study; SI = 0 for contact model (Fig. 8), SI=1 for Dike and Sill models (Fig. 9), SI=2 for Pipe and horizontal/vertical cylinder models (Fig. 10) and SI = 3 for sphere and barrel models (Fig. 11). From the four maps, the depths to magnetic source within the area are categorized in to five (5) sections red colour area less than 100m, blue colour 100m-300m , green colour 300m-500, yellow colour 500m-700m and pink colour greater than 700m respectively. There are positive correlation between obtained Euler depth and Source parameter imaging depth, the depth obtained from SPI ranged from 80m – 742m which are similarly obtained from euler solution. Government and investors should prioritize the prospects zones for further consideration and development. Putting these approaches into effect will aid in the promotion of gold production in the study area and promote sustainable mineral development.

REFERENCES

[1] Murthy, B. S. R. (2007). Airborne geophysics and the indian scenario. J. Ind. Geophysics Miller, H.G. Singh, V.J., (1994). Potential Field tilt - A new concept for location of potential field sources. Applied Geophysics, **32**, 213-217.

[2] Kearey, P. Brooks, M. and Hill, I. (2002). An introduction to geophysical Exploration third Edition.TJ international. 2-160.

[3] Okiwelu, A. A. Ofrey-Kulo, O. and Ude, I. A. (2013). Interpretation of regional magnetic data offshore Niger Delta reveals relationship between deep basement architecture and hydrocarbon target. *Earth Science Research, 2(1)*, 13-32.

[4] Abdullahi H., Bello Yusuf I., Chifu E. N., Maharaz M. N., Ahmad A., Nasiru B., Auwal I., Nasir Y. and Ibrahim A. (2021). Determination of Depth to Basement Using Spectral Analysis of Aeromagnetic Data over Azare Segment of Chad Basin. *Dutse Journal of Pure and Applied Sciences (DUJOPAS),* 7 (4b), 189-202.

[5] Sehsah, H., Eldosouky, A.M., (2020.) Neoproterozoic hybrid forearc – MOR ophiolite belts in the northern Arabian-Nubian Shield: no evidence for back-arc tectonic setting. Int. Geol. Rev. https://doi.org/10.1080/00206814.2020.1836523.

[6] Pham, L.T., Eldosouky, A.M., Melouah, O., Abdelrahman, K., Alzahrani, H., Oliveira, S. P., Andráš, P. (2021). Mapping subsurface structural lineaments using the edge filters of gravity data. *Journal of King Saud University - Science,* 33(8), 101594, ISSN 1018-3647, https://doi.org/10.1016/j.jksus.2021.101594.

[7] Melouah, O., López Steinmetz, R.L., Ebong, E.D., (2021a). Deep crustal architecture of the eastern limit of the West African Craton: Ougarta Range and Western Algerian Sahara. *Journal of Africa Earth Science* 183, 104321. h/ttps://doi.org/10.1016 j. jafrearsci.2021.104321.

[8] Melouah, O., Eldesouky, A.M., Ebong, D.E. (2021b). Crustal architecture, heat transfer modes and geothermal energy potentials of the Algerian Triassic provinces. Geothermics. 96, https://doi.org/10.1016/j.geothermics.2021.102211 102211.

[9] Ahmed, M. E., Sayed, O. E., Ali M. M., Ahlam, A. S., Mohammed, S. F., Kamal, A. and Peter, A. (2021). Structural analysis and basement topography of Gabal Shilman area, South Eastern Desert of Egypt, using aeromagnetic data. *Journal of King Saud University*, 34(2022) 101764.

[10] Sani, A.A. Augie, A.I. and Aku. M.O. (2019). Analysis of Gold Mineral Potentials in Anka Schist Belt, North Western Nigeria Using Aeromagnetic Data Interpretation, *Journal of the Nigerian Association of Mathematical Physics*, 52: 291 – 298

[11] Daniel, A., Owonipa, O.D., (2016). Lineament Mapping and Groundwater Occurrence within the Vicinity of Osara Dam. Itakpe-Okene area, North Central Nigeria, using Landsat Data. Journal of Geosciences and Geomatics 4 (3), 42–52. https://doi.org/10.12691/jgg-4-3-1.

[12] Kankara, I. A. and Darma, M. R. (2016). A Review of Gold Metallurgeny in Nigeria. *Int'l Journal of Research in Chemical, Metallurgical and Civil Engg. (IJRCMCE)* 3 (2). ISSN 2349-1442 EISSN 2349-1450.

[13] Samson, A.O., Akinlolu F. A. and Dieter R. (2014). Mineralogical and Geochemical Characterization of Gold Bearing Quartz Veins and Soils in Parts of Maru Schist Belt Area, Northwestern Nigeria, *Journal of Geological Research,* ID 314214, 17

[14] Adeleke, O.S., Akinlolu F. A. and Dieter R. (2014). Mineralogical and Geochemical Characterization of Gold Bearing Quartz Veins and Soils in Parts of Maru Schist Belt Area, Northwestern Nigeria. *Journal of Geological Research,* 2014, 17. http://dx.doi.org/10.1155/2014/314214

[15] Danbatta, U.A., Abubakar Y.I. and Ibrahim, A.A. (2008). Geochemistry of Gold Deposits in Anka Schist Belt, Northwestern, Nigeria, *Nigerian Journal of Chemical Research,* 13,

[16] Wright, J.B. (1985). Geology and mineral resources of West Africa. George Allen and Unwin, London, 187.

[17] Holt, R., (1982). Geotectonic evolution of the Anka belt in the Precambrian basement complex of Northwestern Nigeria. Unpublished Ph.D. Thesis. Open University, England, 254.

[18] Obaje, N.G. (2009). Geology and Mineral Resources of Nigeria, Lecture Notes in Earth SciencesSpringer-Verlag Berlin Heidelberg, pp. 57-68.

[19] Telford, W.M., Geldart, L.P. and Sheriff, R.E. (1990). Applied Geophysics Second Edition. Cambridge University Press.

[20] Leu, L. (1982) Use of Reduction-to-the-Equator Process for Magnetic Data Interpretation. Geophysics, 47, 445.

[21] Yaoguo, I. and Dougla, W. O. (1998). Separation of Regional and Residual Magnetic field data, Annual international meeting society of exploration geophysicists. 63(2), 431-439.

[22] Miller, H.G. Singh, V.J., (1994). Potential Field tilt - A new concept for location of potential field sources. Applied Geophysics, **32**, 213-217.

[23] Holden, E.-J. (2010). Detection of regions of structural complexity within aeromagnetic data using image analysis. In *2010 25th International Conference of Image and Vision Computing New Zealand* 1–8 IEEE.

[24] Reid, A. B., Allsop, J. M., Granser, H., Millett, A. J. T. & Somerton, I. W. (1990). Magnetic interpretation in three dimensions using Euler deconvolution. *Geophysics* 55, 80–91

[25] Thurston, J.B., and Smith, R.S., (1997), Automatic conversion of magnetic data to depth, dip and susceptibility contrast using the SPITM method, Geophysics, 62, 807-813.